VECTOR ANALYSIS OF ICE PETROGRAPHIC DATA

M.G. Ferrick, K.J. Claffey and J.A. Richter-Menge

USA Cold Regions Research and Engineering Laboratory
Hanover, NH 03755-1290

ABSTRACT

In this paper we develop a quantitative analysis of uniaxial crystal orientation data. Though the method is general, we focus on the application of the analysis to ice fabrics. The crystal orientation data are represented as points on the surface of a unit sphere. An orthogonal least-squares error measure is used to develop equations that define the closest plane and line through the data while retaining all coordinate directions as independent variables. For comparison, a parallel development is presented of the standard dependent variable least-squares determination of the best plane. The orthogonal error measure quantifies the goodness-of-fit to the data of all approximate representations. Finally, a technique is developed to generalize from the standard Schmidt net presentation of data in the xy-plane to a presentation in any of the three planes defined by the Cartesian coordinate system.

INTRODUCTION

Ice crystals are uniaxial, and crystal orientation measurements describe the optical c-axis orientation of each crystal in a particular sample. Research in ice mechanics (e.g., Richter-Menge et al. 1986) has shown that there is a strong relationship between the behavior of ice and its crystal structure, including the relative orientation of the crystals. Environmental conditions at the time of formation determine the ice structure. Random c-axis orientation is typical near the top surface of a sea ice sheet. Once a cover has formed, the ice structure is characterized by long vertical columns that extend downward in the growth direction of the ice sheet, a result of quiescent, unidirectional growth. Under these conditions a selective growth process occurs, and the c-axis is primarily oriented in the horizontal plane of the ice sheet (Weeks and Ackley 1982). In the presence of a predominant current direction, strong c-axis alignment develops in the direction of the current with decreasing scatter as ice thickness increases (Weeks and Gow 1978). In this case the ice structure results in a material that behaves anisotropically in all directions. The analysis of uniaxial compression data on first-year sea ice (Richter-Menge et al. 1986, Wang 1979) has indicated a strong dependence of peak compressive strength on c-axis alignment and direction. The angle between an applied load and the dominant c-axis direction, and the angle between the load and the direction of crystal elongation are of particular interest. Therefore, to interpret data from mechanical property tests it is necessary to define the relative orientation of the ice fabric.

Langway (1958) describes techniques for obtaining ice crystal orientation data using a Rigsby universal stage. The techniques used in the analysis of ice fabrics were originally developed in structural petrology (Fairbairn 1949, Knopf and Ingerson 1938, Turner and Weiss 1963). One orientation measurement is made for each ice crystal in a sample, and these data are plotted on a Schmidt equal area net (Fig. 1). The points on the net are an orientation diagram, and this representation reduces the dimension of the hemisphere and of any plane or line by one. The pole of a plane is the point of intersection with the hemisphere of a line normal to the plane through the origin. The dimension of a plane can be reduced again by representing it with its pole. An orientation diagram of a

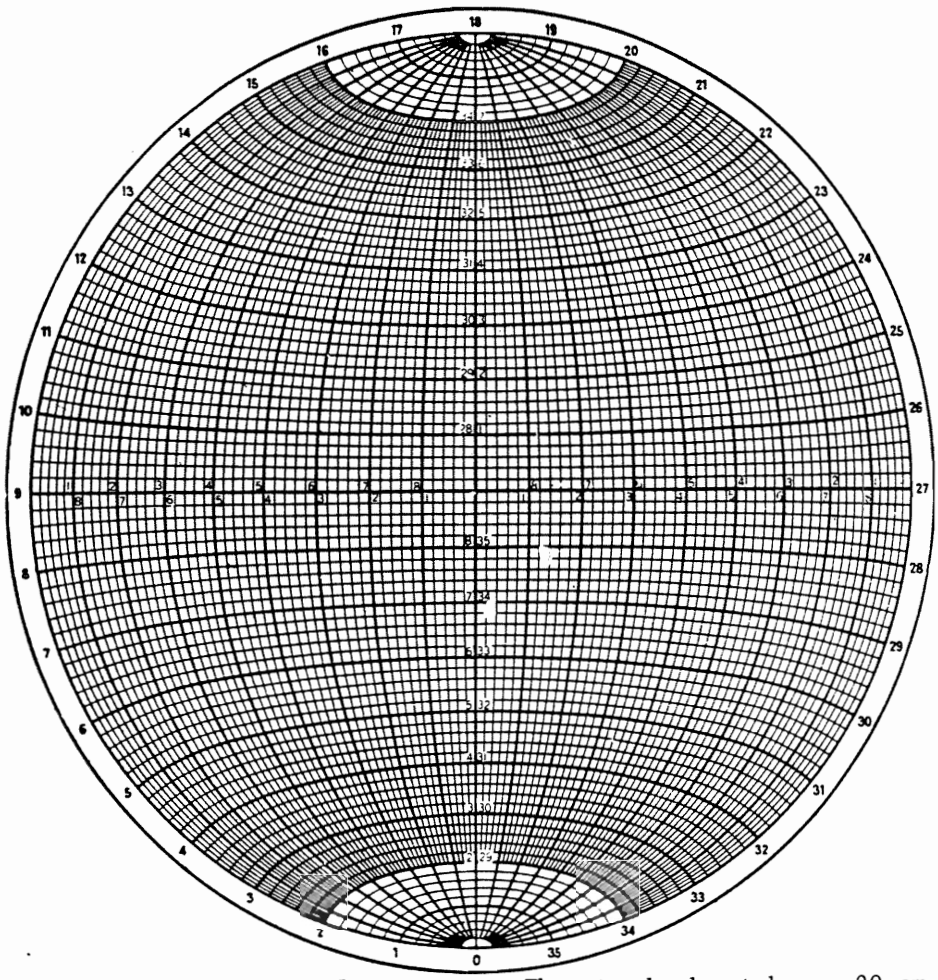

Figure 1: Schmidt equal area net. The standard net has a 20 cm diameter.

crystal fabric may indicate a random or a patterned structure, depending on the dominant features of the orientation diagram. A random orientation refers to a lack of local concentration of the plotted points and represents an isotropic material. In this configuration there is an equal probability of finding points in equal area elements anywhere on the net. In contrast, the most significant feature of an anisotropic material is the preferred orientation indicated by the grouping of points on the net. A "girdle" corresponds to data that cluster about a great circle of the net, indicating a preferred planar orientation of the c-axes. The pole of this great circle is in a sparsely populated area termed the girdle axis. A single area of high concentration indicates a linear preferred orientation of the crystals in the fabric. The statistical significance of the fabric diagram increases if the main features (maxima/girdles) are reproducible in different comparable samples from the same homogeneous body. The primary weakness of this widely accepted methodology is in the qualitative interpretation of the data.

Our analysis provides quantitative measures of both the planar and linear structure of materials with uniaxial crystals using standard orientation data obtained with a universal stage. For each ice crystal, the orientation of the c-axis is represented by a line passing through the origin of a three-dimensional coordinate system. Because these lines are symmetric about the origin, and following standard practice, the orientation of each c-axis is represented by a vector from the origin with the direction of the line in the half-space below the xy-plane. For equal representation of each crystal the vectors must have the same length, and a unit length was chosen for convenience. The vectors then yield an array of points on the surface of a hemisphere of unit radius. A plane that passes through the origin is obtained that minimizes the sum of the squared normal distances from these points to the plane. We show that the dominant c-axis orientation lies in this plane and obtain this linear orientation. The corresponding measures of spread quantify the planar and linear directional characteristics of the c-axes of crystals in an

ice sample. In a companion paper (Claffey et al. 1989) we give a detailed description of the algorithm and program that implement this analysis.

BACKGROUND

A c-axis orientation measurement of an ice crystal with the Rigsby universal stage (Langway 1958) yields an azimuth angle, an inclination angle, the direction of inclination as right or left, and the type of measurement as polar or equatorial. The azimuth angle measures the rotation of the crystal about the z-axis that places the c-axis in the xz-plane. The zero azimuth can be chosen arbitrarily, depending on the requirements of the analysis. Beginning with the crystal in the xz-plane, the inclination angle is found by rotation about the y-axis. An inclination angle of zero is defined as the angle where the c-axis of the crystal is parallel to the x-axis. From this position the crystal is tilted either to the right or the left, and inclination angle is the direction and angle of tilt with the x-axis. The optical axis of a crystal that has been aligned parallel to the z-axis is termed a polar measurement, and parallel to the x-axis is an equatorial measurement. The measured inclination angle must be corrected for the optical error caused by the difference in the refractive indices of air and ice. The relationship between the corrected inclination, I, and the measured inclination, I_m, depends on the measurement type and can be expressed (Kamb 1962) as

$$I = \begin{cases} 1.04\ I_m & ;\ \text{equatorial} \\ \sin^{-1}\left(\frac{1}{1.31}\sin I_m\right) & ;\ \text{polar} \end{cases} \qquad (1)$$

Taken together, the azimuth and inclination measurements define the orientation of the optical axis of an ice crystal in three-dimensional space. The surface of the lower hemisphere of a sphere of unit radius is represented in two dimensions with the Schmidt equal area net (Fig. 1). The crystal orientation data plotted on this net represent the points of intersection of the unit vectors of individual crystals and the surface of the hemisphere. The Schmidt net is composed of two sets of arcs. The set that crosses the x-axis represents the intersection of great circle planes passing through the y-axis with the unit sphere. These arcs are meridians of the net that correspond to inclination angles between -90° and +90°, representing the angle between the lower half of the yz-plane and the plane of the arc. The labels on the x-axis correspond to polar or equatorial crystal orientation with right or left tilt. The set of arcs that cross the y-axis are parallels of the net, and represent the intersection of planes parallel to the xz-plane with the sphere. The points of intersection of these arcs with the perimeter of the net represent the azimuth angle, and the notation on the net is in degrees of angle. A unit area in any position on the net corresponds to a unit area on the surface of the hemisphere from which the net was derived. The Schmidt net eliminates nearly all areal distortion, and shows the relative spatial concentration of the measured data. Additional details that are needed for plotting petrographic data on the Schmidt net are given by Langway (1958).

DATA TRANSFORMATION TO CARTESIAN COORDINATES

We will view both the data and the results of our analysis on the Schmidt net. Therefore, we must obtain Cartesian coordinates on the net that represent the petrographic data from the universal stage. In addition, the position on the unit hemisphere of each crystal in a sample is required for the analysis, and we will use a three-dimensional Cartesian coordinate system to locate each point (Fig. 2).

The initial step in finding the net coordinates is to obtain polar coordinates (r,θ) on the net for each point. Defining the positive x-axis as the zero azimuth, we obtain θ directly as the recorded azimuth. The inclination angle is used to find the radial coordinate. For polar crystals the inclination angle, I, is the angular displacement measured from the yz-plane that places the c-axis parallel to the z-axis. Polar crystals with right tilt yield positive I, and polar, left crystals have negative I. Equatorial measurements of I are angular displacements measured from the x-axis that place the c-axis

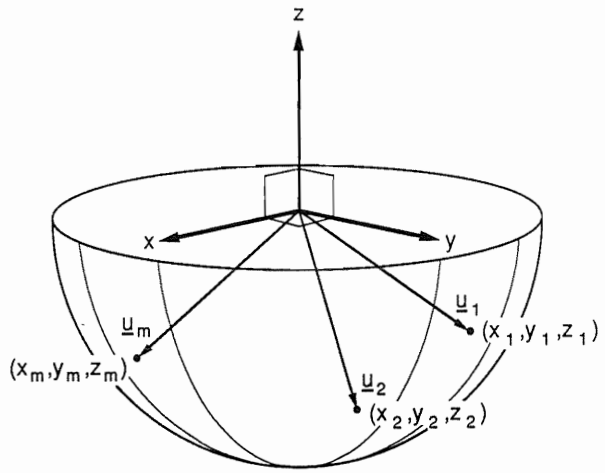

Figure 2: Sketch of unit vectors 1,2,...,m,...N representing the c-axis orientations of ice crystals in a sample. The hemisphere, $z \leq 0$, is shown by convention.

parallel to the x-axis. Since the inclination angle on the net is from the z-axis, the complement of I is required. Equatorial angles with right tilt are negative, and left tilt angles are positive. Summarizing, we obtain the angle ϕ measured from the z-axis as

$$\phi = \begin{cases} -I & ; \quad \text{polar, left} \\ I & ; \quad \text{polar, right} \\ (90°-I) & ; \quad \text{equatorial, left} \\ -(90°-I) & ; \quad \text{equatorial, right} \end{cases} \tag{2}$$

The distance from the origin of the Schmidt net r can be determined (Knopf and Ingerson 1938) as

$$r = (2a)\sin(\phi/2) \tag{3}$$

where $a = 0.70711R$, and R is the radius of the net. If ϕ is negative the radial coordinate will also be negative. In these cases r is taken as positive and the azimuth is adjusted by 180°. The equivalent Cartesian coordinates are then obtained directly as

$$\begin{aligned} x &= r\cos\theta \\ y &= r\sin\theta \end{aligned} \tag{4}$$

The initial step in finding the three-dimensional Cartesian coordinates is to represent each point in spherical coordinates (ρ,ϕ,θ). Because each crystal is represented by a unit vector, the radius $\rho = 1$ for all the data. The polar angle θ, measured from the positive x-axis with a range of 0° to 360°, is again simply the recorded azimuth angle when the zero azimuth is defined as the positive x-axis. The angle ϕ is measured from the positive z-axis with a range of 0° to 180°, and can be obtained from the inclination data. The inclination angle was measured from the negative z-axis for polar crystals and from the xy-plane for equatorial crystals, and ϕ is determined as

$$\phi = \begin{cases} (180°-I) & ; \quad \text{polar} \\ (90°+I) & ; \quad \text{equatorial} \end{cases} \tag{5}$$

With the spherical coordinates specified, the equivalent Cartesian coordinates are obtained directly as

$$\begin{aligned} x &= \rho\sin\phi\cos\theta \\ y &= \rho\sin\phi\sin\theta \\ z &= \rho\cos\phi \end{aligned} \tag{6}$$

DETERMINATION OF THE BEST PLANE BY ORTHOGONAL LEAST-SQUARES

In this section we consider the case where the fabric data are roughly in the form of a girdle on the Schmidt net. The problem is to find the plane of best fit to these data that passes through the origin of the hemisphere, and to provide a quantitative measure of the quality of the fit. The form of the equation of a plane through the origin is

$$f(x,y,z) = Ax + By + Cz = 0 \tag{7}$$

Therefore, we choose the function $F(x,y,z) = F(x,y,z;c_1,c_2,c_3)$ with this same form and depending linearly on parameters c_1, c_2, c_3 as

$$F(x,y,z) = c_1\phi_1 + c_2\phi_2 + c_3\phi_3 = \sum_{i=1}^{3} c_i\phi_i = 0 \tag{8}$$

where ϕ_i are a specified set of functions and the c_i are parameters to be determined. Comparing the form of (7) and (8), we specify a mutually orthogonal set of functions ϕ_i as

$$\phi_1 = x,\ \phi_2 = y,\ \phi_3 = z \tag{9}$$

The number of the data points used to fit the plane should be much larger than 3. For a data point located at (x_m,y_m,z_m) we can evaluate $F(x_m,y_m,z_m;c_1,c_2,c_3) = F_m$ with (8) as

$$F_m = c_1x_m + c_2y_m + c_3z_m \tag{10}$$

The unit normal to the plane $F(x,y,z) = 0$ is

$$\underline{n} = c_1\,\underline{i} + c_2\,\underline{j} + c_3\,\underline{k} \tag{11}$$

The unit vector representing the c-axis of the mth crystal in a sample (Fig. 3) is

$$\underline{u}_m = x_m\,\underline{i} + y_m\,\underline{j} + z_m\,\underline{k} = \phi_{1_m}\,\underline{i} + \phi_{2_m}\,\underline{j} + \phi_{3_m}\,\underline{k} \tag{12}$$

The vector $\tilde{\underline{w}}_m$ is the projection of $\underline{u}_m$ onto $\underline{n}$ (Fig. 3), representing the normal vector from the point to the plane

$$\tilde{\underline{w}}_m = \left(\frac{\underline{u}_m\cdot\underline{n}}{\underline{n}\cdot\underline{n}}\right)\underline{n} = (\underline{u}_m\cdot\underline{n})\underline{n} \tag{13}$$

Throughout this development the notation (~) over a vector indicates that it does not have unit length. The normal distance from the point to the plane is represented by the length of $\tilde{\underline{w}}_m$

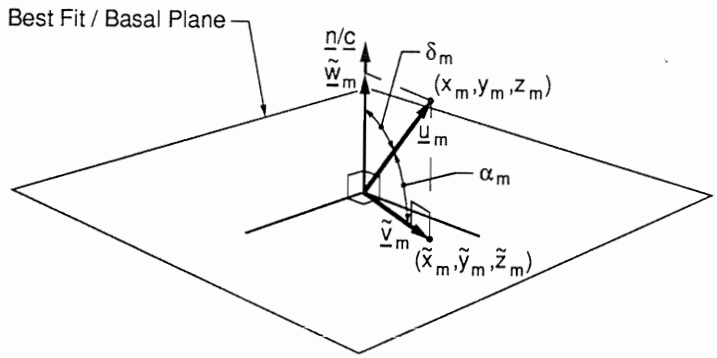

Figure 3: Sketch of the unit vector $\underline{u}_m$ representing the mth crystal in an ice sample and its projections $\tilde{\underline{v}}_m$ onto the best-fit plane or the basal plane and $\tilde{\underline{w}}_m$ onto $\underline{n}$ or $\underline{c}$ the unit normal vector to the corresponding plane.

$$|\tilde{\underline{w}}_m| = (\tilde{\underline{w}}_m \cdot \tilde{\underline{w}}_m)^{\frac{1}{2}} = (\underline{u}_m \cdot \underline{n}) = c_1 x_m + c_2 y_m + c_3 z_m \tag{14}$$

and with (10) we observe that

$$\text{and} \quad \begin{aligned} |\tilde{\underline{w}}_m| &= F_m \ , \quad |F_m| \le 1 \\ \tilde{\underline{w}}_m &= F_m \, \underline{n} \end{aligned} \tag{15}$$

The normal distance between the mth data point and the plane of best fit described by $F(x,y,z;c_1,c_2,c_3) = 0$ is F_m, and the sign F_m distinguishes distances on opposite sides of the plane.

We want to choose the c_i values that specify the plane so that the normal distances between each of the N crystals in a sample and the plane

$$d_m = F_m \qquad m = 1, 2, \ldots, N \tag{16}$$

are as small as possible, and some norm of the N-vector $\underline{d} = (d_1, d_2, \ldots, d_N)^T$ is minimized. The vector $\underline{d}$ represents the individual normal distances from the data to the plane and serves as an "error vector." Because we consider distances normal to a plane, the hemisphere in which the data appears is arbitrary. This fact allows us to follow the standard practice of using the hemisphere below the xy-plane. We will seek a least-squares fit of the data to the plane, and will use the 2-norm

$$||\underline{d}||_2 = \left(\sum_{m=1}^{N} |d_m|^2 \right)^{\frac{1}{2}} \tag{17}$$

The square root is a monotone nondecreasing function, and minimizing $||\underline{d}||_2$ is equivalent to minimizing $||\underline{d}||_2^2$. Next, we define

$$E(c_1,c_2,c_3) = ||\underline{d}||_2^2 = \sum_{m=1}^{N} |d_m|^2 = \sum_{m=1}^{N} (F(x_m,y_m,z_m;c_1,c_2,c_3))^2 \tag{18}$$

where the absolute value sign is deleted because F_m is squared. The gradient of E must vanish at (c_1^*,c_2^*,c_3^*) corresponding to the plane of best fit

$$\nabla E(c_1^*,c_2^*,c_3^*) = \underline{0} \tag{19}$$

The orthogonal projection of $\underline{u}_m$ in the best fit plane is represented by $\tilde{\underline{v}}_m$ (Fig. 3), and

$$\tilde{\underline{v}}_m = \underline{u}_m - \tilde{\underline{w}}_m = \tilde{x}_m \, \underline{i} + \tilde{y}_m \, \underline{j} + \tilde{z}_m \, \underline{k} = \tilde{\phi}_{1_m} \underline{i} + \tilde{\phi}_{2_m} \, \underline{j} + \tilde{\phi}_{3_m} \underline{k} \tag{20}$$

This vector joins the origin and the point $(\tilde{x}_m,\tilde{y}_m,\tilde{z}_m)$, the orthogonal projection of (x_m,y_m,z_m) in the plane. The vector $\tilde{\underline{v}}_m$ is the closest representation of $\underline{u}_m$ in the plane. From (20) we can determine $\tilde{x}_m,\tilde{y}_m,\tilde{z}_m$ as

$$\left.\begin{aligned} \tilde{x}_m &= x_m - d_m c_1 \\ \tilde{y}_m &= y_m - d_m c_2 \\ \tilde{z}_m &= z_m - d_m c_3 \end{aligned}\right\} \quad \text{for } m = 1,2,\ldots,N$$

$$\text{or} \qquad \tilde{\phi}_{im} = \phi_{im} - d_m c_i \qquad \text{for } i = 1,2,3 \tag{21}$$

where ϕ_{im} and $\tilde{\phi}_{im}$ represent elements of N-dimensional vectors $\underline{\phi}_i$ and $\tilde{\underline{\phi}}_i$, respectively.

We will now differentiate (18), noting that the normal distance F_m is a composite function, $F_m[F(c_i)]$, and taking $h[F(c_i)] = F_m^2$,

$$\frac{\partial h}{\partial c_i} = h'(F) \frac{\partial F}{\partial c_i} = 2 \, F_m \, \tilde{\phi}_{im} \tag{22}$$

Then, using (22) we rewrite (19) as

$$\nabla E(c_1^*, c_2^*, c_3^*) = 2 \sum_{m=1}^{N} d_m \tilde{\phi}_{im} = 0$$

which written in vector form is

$$\sum_{m=1}^{N} d_m \tilde{\phi}_{im} = \underline{d}^T \cdot \tilde{\underline{\phi}}_i = 0 \qquad \text{for } i = 1,2,3 \tag{23}$$

Equations (23) state that the error vector is orthogonal to each of the N-vectors $\tilde{\underline{\phi}}_i$, and are termed the normal equations. Therefore, the error vector is orthogonal to all possible approximating functions composed of linear combinations of $\tilde{\underline{\phi}}_i$, specifically

$$\underline{d}^T \cdot (c_1 \tilde{\underline{\phi}}_1 + c_2 \tilde{\underline{\phi}}_2 + c_3 \tilde{\underline{\phi}}_3) = 0 \qquad \text{for all } c_1,\ c_2,\ c_3 \tag{24}$$

where the vector $(c_1 \tilde{\underline{\phi}}_1 + c_2 \tilde{\underline{\phi}}_2 + c_3 \tilde{\underline{\phi}}_3)$ is the orthogonal projection of the data onto the plane spanned by the vectors $\tilde{\underline{\phi}}_1$, $\tilde{\underline{\phi}}_2$, $\tilde{\underline{\phi}}_3$.

Restating (21) in vector notation and inserting into (23) we obtain

$$\underline{d}^T \cdot (\underline{\phi}_i - c_i \underline{d}) = 0$$

or

$$\underline{d}^T \cdot \underline{\phi}_i = (\underline{d}^T \cdot \underline{d})\ c_i = |\underline{d}|^2\ c_i \tag{25}$$

Rewriting the left side of (25) yields

$$\sum_{j=1}^{3} [\underline{\phi}_j^T \cdot \underline{\phi}_i]\ c_j = |\underline{d}|^2\ c_i \qquad , \qquad \text{for } i = 1,2,3 \tag{26}$$

Setting the constant $|\underline{d}|^2 = \lambda$ we observe that (26) has the form of an eigenvalue problem,

$$A\underline{c} = \lambda \underline{c} \tag{27}$$

where the matrix

$$A = \sum_{j=1}^{3} [\underline{\phi}_j^T \cdot \underline{\phi}_i]$$

As defined, the eigenvalue λ is the sum of the squared distances of the data from the plane. Equation (27) in homogeneous form,

$$(A - \lambda I)\ \underline{c} = \underline{0}$$

indicates that nontrivial solutions exist if and only if

$$\det(A - \lambda I) = 0 \quad . \tag{28}$$

The determinant given in (28) yields a cubic equation in the form

$$\lambda^3 + p\lambda^2 + q\lambda + r = 0 \tag{29}$$

Following Beyer (1987) we obtain the solution as

$$\begin{aligned} \lambda_1 &= m\cos\beta - p/3 \\ \lambda_2 &= m\cos(\beta + 2\pi/3) - p/3 \\ \lambda_3 &= m\cos(\beta + 4\pi/3) - p/3 \end{aligned} \tag{30}$$

where

$$\beta = (1/3)\cos^{-1}\left[\frac{3b}{am}\right]$$

$$m = 2\sqrt{-a/3}$$

$$a = (1/3)(3q-p^2)$$

$$b = (1/27)(2p^3 - 9pq + 27r)$$

The spectral theorem (Shields 1968) states that because A is a symmetric matrix it is similar to a diagonal matrix B composed of the eigenvalues of A, and therefore the eigenvalues of A are real. Similar matrices have the same trace and the same determinant. The trace of a matrix is the sum of the elements on the principal diagonal. The elements a_{11}, a_{22} and a_{33} of matrix A represent the sum of the squares of the x-, y-, and z-coordinates, respectively, of all the data in a sample. These values represent the squares of distances between the data and the three planes defined by the coordinate axes. Because each crystal is represented by a unit vector,

$$\mathrm{tr}(A) = \sum_{i=1}^{3} a_{ii} = N = \mathrm{tr}(B) = \sum_{i=1}^{3} b_{ii} = \sum_{i=1}^{3} \lambda_i \tag{31}$$

indicating that the sum of the eigenvalues is N, the total number of crystals in the sample. The determinants of A and B are the product of the eigenvalues.

Eigenvectors of a real symmetric matrix corresponding to different eigenvalues are orthogonal, and because the eigenvalues are real, the eigenvectors can be taken to be real. The vector $\underline{v}$ is an eigenvector for A belonging to the eigenvalue λ if

$$A\underline{v} = \lambda\underline{v} \quad \text{and} \quad \underline{v} \neq \underline{0} \tag{32}$$

The lengths of these eigenvectors are arbitrary, and we normalize them to unit length to obtain an orthonormal basis in three-dimensional space. Each eigenvector represents the unit normal to a plane, and the corresponding eigenvalue gives the sum of the squared normal deviations of the data from that plane. The minimum eigenvalue defines the plane of best least-squares fit to the data, and the higher eigenvalues are associated with the remaining mutually orthogonal planes through the origin. With the origin fixed, the eigenvector basis represents a coordinate system that is rotated relative to the coordinate axes. The eigenvectors written in columns form the matrix P. The elements of P are the direction cosines between each eigenvector and the coordinate axes. For example, the angles α_i between the eigenvector $\underline{n}$ and the axes are obtained as

$$\alpha_i = \cos^{-1}(\underline{n}\cdot\underline{\phi}_i) \quad , \quad i = 1, 2, 3 \tag{33}$$

where $\underline{\phi}_1 = \underline{i}$, $\underline{\phi}_2 = \underline{j}$ and $\underline{\phi}_3 = \underline{k}$. Because the columns of P are orthonormal, P is an orthogonal matrix and $P^{-1} = P^T$, det $P = \pm 1$. Matrices A and B are related through P as

$$B = P^{-1}AP \tag{34}$$

The sum of the squared normal distances between the data and the best plane, given by λ_{min}, provides a measure of the planar structure of an ice sample. We define the mean normal error e_n as the average squared normal distance between individual crystals and the best plane, and

$$e_n = \frac{\lambda}{N} \tag{35}$$

Values of e_n approaching zero indicate an increasingly planar ice structure. A visual representation of the error is obtained from the angle α_m between an individual crystal and its projection in the best plane (Fig. 3),

$$\alpha_m = |\pi/2 - \cos^{-1}(\underline{u}_m\cdot\underline{n})| \tag{36}$$

The absolute value in (36) is needed if the angle between $\underline{u}_m$ and $\underline{n}$ is greater than $\pi/2$.

Then, the average angular deviation $\bar{\alpha}$ between the data and the best plane is a parameter we term the planar spread that can be readily determined and understood:

$$\bar{\alpha} = \frac{1}{N} \sum_{m=1}^{N} \alpha_m \tag{37}$$

A small planar spread indicates a small mean angle between the crystals in a sample and the plane.

DEVELOPMENT OF DEPENDENT VARIABLE LEAST-SQUARES SOLUTIONS

We will now parallel the development of the previous section to obtain a set of dependent variable least-squares solutions to the problem of fitting a plane to three-dimensional data. Arbitrarily selecting z as the dependent variable, we rewrite (8) as

$$z = F(x,y) = c_1 \phi_1 + c_2 \phi_2 \tag{38}$$

where $\phi_1 = x$ and $\phi_2 = y$. The coefficients c_1 and c_2 are chosen so that the deviations d_m are as small as possible,

$$d_m = r_m - F(x_m, y_m; c_1, c_2) \quad , \tag{39}$$

in which r_m is z_m, the z-value of the mth point, and $F(x_m,y_m;c_1,c_2)$ is the corresponding z-value in the plane of best fit. Again, we use the 2-norm of the vector $\underline{d}$ to measure error, and write an equation for the parameter E as

$$E(c_1,c_2) = ||d||_2^2 = \sum_{m=1}^{N} [r_m - F(x_m, y_m; c_1, c_2)]^2 \tag{40}$$

Taking the gradient of E and setting it to zero yields the normal equations

$$\sum_{m=1}^{N} [r_m - F(x_m, y_m; c_1, c_2)] \phi_{im} = 0 \quad , \quad i = 1,2 \tag{41}$$

or

$$\underline{d}^T \cdot \underline{\phi}_i = 0$$

indicating that the error vector is normal to each vector $\underline{\phi}_i$. Now, inserting (38) and rewriting the normal equations in vector form we obtain a pair of linear equations:

$$\sum_{j=1}^{2} [\underline{\phi}_j^T \cdot \underline{\phi}_i] \underline{c}_j = \underline{r}^T \cdot \underline{\phi}_i \qquad i = 1,2 \tag{42}$$

The vector normal to the plane that minimizes the sum of the squared z-distances with the data is

$$\tilde{\underline{n}} = c_1 \underline{i} + \underline{c}_2 \underline{j} - \underline{k}$$

or in the form of a unit vector,

$$\underline{n} = \frac{1}{(c_1^2 + c_2^2 + 1)^{1/2}} (c_1 \underline{i} + c_2 \underline{j} - \underline{k}) \tag{43}$$

The normal distances between the data and the plane represented by $\underline{n}$ can then be determined using (14) as

$$|\tilde{w}_m| = (\underline{u}_m \cdot \underline{n}) = \frac{(c_1 x_m + c_2 y_m - z_m)}{(c_1^2 + c_2^2 + 1)^{1/2}} \quad \text{for} \quad m = 1,2,\ldots, N \tag{44}$$

The sum of the squared normal distances given in (44) is directly comparable to the minimum eigenvalue obtained in the previous section. The planes that minimize the squared x-deviations and squared y-deviations are obtained by interchanging the roles of $\underline{\phi}_1$, $\underline{\phi}_2$ and $\underline{r}$ above, and repeating the analysis.

ALIGNMENT OF THE C-AXES IN A SINGLE DIRECTION

Alignment of the c-axes within the plane indicates a linear preferred orientation of the ice crystals in a sample, and suggests the need to determine the predominant optical axis of the fabric. We will locate this linear orientation by following a development parallel to that used to determine the best plane. The unit vector $\underline{c}$ represents the unknown preferred c-axis orientation of the crystals in a sample, and is expressed as

$$\underline{c} = c_1' \underline{i} + c_2' \underline{j} + c_3' \underline{k} \tag{45}$$

where the primes distinguish these coefficients from those of the unit vector $\underline{n}$ given in (11). The plane through the origin that is normal to $\underline{c}$ represents the predominant basal plane orientation of the crystals in the sample and is described by

$$F(x,y,z;\ c_1',c_2',c_3') = c_1'x + c_2'y + c_3'z = 0 \tag{46}$$

As before, the unit vector $\underline{u}_m$ represents the mth crystal orientation and intersects the unit hemisphere at (x_m,y_m,z_m). In order to take advantage of the detail given in the previous development, the vector projections of $\underline{u}_m$ onto the plane and its normal vector are again $\tilde{\underline{v}}_m$ and $\tilde{\underline{w}}_m$, respectively. These vectors have the same meaning but are not the same vectors as those used in finding the best plane. Then, with $\underline{c}$ replacing $\underline{n}$ and a different normal plane, Figure 3 represents our present condition.

When searching for the plane that best represented the unit vectors $\underline{u}_m$, we sought to minimize the squared normal distance $|\tilde{\underline{w}}_m|$. However, the closest representation of $\underline{u}_m$ by the unit vector $\underline{c}$ requires that we maximize the sum of the squares of the lengths of $\tilde{\underline{w}}_m$. The basal plane is then the plane of maximum squared normal error with the data. Each step in the previous development applies except that c_i is replaced by c_i'. Note that the matrix A in (27) is unchanged because it depends only on the coefficients of the intersections of the individual unit vectors $\underline{u}_m$ with the unit hemisphere. Therefore, we are solving the same eigenvalue problem as before. The eigenvectors obtained in (31) are orthogonal, and $\underline{c}$ is contained in the best plane. The third eigenvector $\underline{s}$ together with $\underline{c}$ form the plane of best fit to the c-axes, and $\underline{s}$ and $\underline{n}$ form the predominant basal plane (Fig. 4). The direction cosines of the angles between the preferred linear orientation and the coordinate axes are given in matrix P, and the angles can be obtained from (33) with $\underline{c}$ replacing $\underline{n}$.

As with the plane, λ_{max} is a measure of the linear structure of the ice sample. In this case values of e_n obtained with λ_{max} that approach 1 indicate a more linear structure. Again using angles to visualize error, the angle δ_m between an individual (crystal) vector and its projection onto $\underline{c}$ (Fig. 3) is obtained as

$$\delta_m = \cos^{-1} (\underline{u}_m \cdot \underline{c}) \tag{47}$$

and the average angle $\bar{\delta}$ between the data and $\underline{c}$ is

$$\bar{\delta} = \frac{1}{N} \sum_{m=1}^{N} \delta_m \tag{48}$$

The parameter $\bar{\delta}$ is termed the linear spread, and a small $\bar{\delta}$ indicates that the angles between the preferred orientation and the data are also small.

If the c-axis data from a given sample are sufficiently aligned, the mechanical properties of the ice will be affected. If $\underline{\sigma}$ is a unit vector in the direction of an applied force, the angle σ_c between the force and the dominant c-axis direction is

$$\sigma_c = \cos^{-1}(\underline{\sigma} \cdot \underline{c}) \tag{49}$$

and the complement of σ_c is the angle between the load and the basal plane (Fig. 4). For a columnar ice sample $\underline{n}$ gives the predominant direction of crystal elongation and growth. The angle σ_z between the load and the vector $\underline{n}$ also affects the mechanical properties of the ice (Richter-Menge et al., 1987), and is obtained as

$$\sigma_z = \cos^{-1} (\underline{\sigma} \cdot \underline{n}) \tag{50}$$

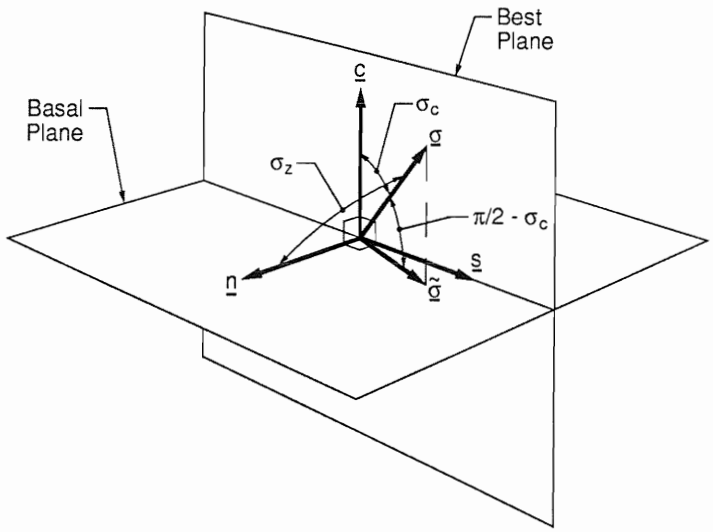

Figure 4: Definition sketch of the angles σ_c and σ_z. The unit vectors $\underline{n}$ and $\underline{s}$ provide the predominant orientation of the basal plane of an ice sample, $\underline{\sigma}$ is a unit vector representing the direction of load application on the sample, $\tilde{\underline{\sigma}}$ is the projection of this vector onto the basal plane, $\underline{c}$ is the unit vector representing the linear preferred c-axis orientation of the ice fabric, σ_c is the angle between the applied load and the preferred orientation, and σ_z is the angle between the load and the long axis of the columnar crystals of an ice sample, represented by $\underline{n}$.

SCHMIDT NET REPRESENTATIONS

The results of the analysis of an ice sample are presented together with the data on the Schmidt net. Planes that pass through the origin, described by (7), intersect the unit sphere as a great circle. The part of the great circle below the xy-plane is drawn on the Schmidt net. With $\rho = 1$, (6) is substituted into (7) and solved for ϕ to obtain

$$\phi = \tan^{-1}\left(\frac{-c_3}{c_1 \cos\theta + c_2 \sin\theta}\right) \tag{51}$$

where θ is incremented in arbitrary steps from 0° to 360°. We obtain polar coordinates on the net from the spherical coordinates with (3), and a final transformation with (4) yields a discrete representation in Cartesian coordinates of the great circle on the net. The requirement of $z \leq 0$ in (6) identifies the points of intersection in the lower hemisphere. Experience indicates that 0.5° increments of θ yield a smooth curve on the net.

The unit normal through the origin to the plane of best fit, termed the pole vector, intersects the unit hemisphere at a point with coordinates (x_p, y_p, z_p) or (c_1, c_2, c_3). Inverting (6) we obtain the spherical coordinates of this point as

$$\phi = \cos^{-1}(c_3)$$
$$\theta = \tan^{-1}\left(\frac{c_2}{c_1}\right) \tag{52}$$

There are two values of θ in the range $0° \leq \theta < 360°$ that have the same tangent. If the value of $x=c_1$ is negative, θ falls in the 2nd or 3rd quadrant and the calculated angle is adjusted by adding 180°. Again, the polar coordinate r on the net is obtained from (3), and the Cartesian coordinates of the pole on the net are found from (4). Similarly, the Cartesian coordinates of the vector representing the intersection of the preferred linear orientation and the unit hemisphere are known from (42). The determination of the Schmidt net coordinates of $\underline{c}$ follows the same procedure as for the pole vector with (c_1, c_2, c_3) in (52) replaced by (c_1', c_2', c_3'). The intercept of the linear orientation vector must fall on that of the great circle of the best planar fit.

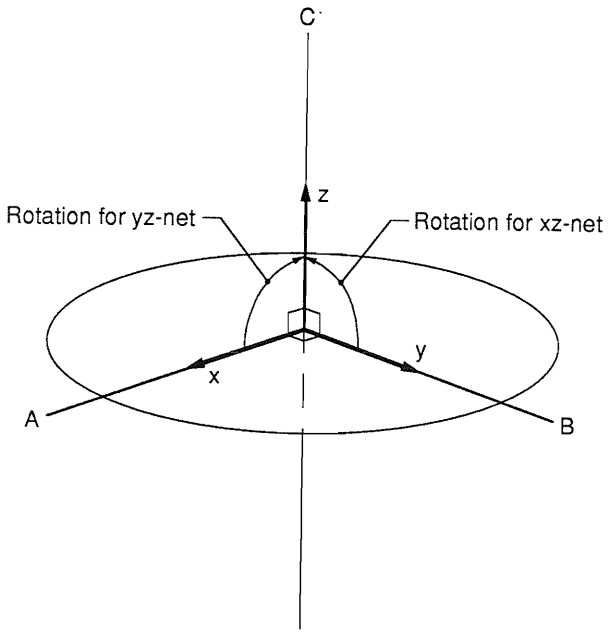

Figure 5: Diagram of rotations of the (x,y,z) coordinate system relative to the fixed (A,B,C) Cartesian coordinate system for analysis of various Schmidt net representations of corresponding data hemispheres.

The linear dimensions on the periphery of the Schmidt net are distorted, and it is difficult to judge normal distances between the data in this region and the trace of the best plane. Also, points that appear directly across the net from each other represent crystals with close planar alignment. For these reasons it is frequently advantageous to view the data on Schmidt nets drawn on alternative planes. With the xy-, xz-, and yz-planes for mapping, the location of the data on the net changes and different views of the structure of the material are available, minimizing the importance of net distortion and measurement accuracy limitations by providing several views of the grouping of crystals. We will use a Cartesian coordinate system fixed in space (A,B,C) and always view the data by looking down on the AB-plane (Fig. 5). The net represents the hemisphere below this plane with $-1 \leq C \leq 0$, We obtain the correct viewing plane by rotating the (x,y,z) system relative to the (A,B,C) system while keeping one axis fixed.

Recall that the line segment from the origin chosen to represent a given crystal was originally selected based on the requirement that $z \leq 0$ at the intersection with the unit sphere. This more general capability requires that line segment selection depend on the hemisphere being studied so that each crystal is represented. For the standard data presentation in the xy-plane, (A,B,C) = (x,y,z). To view the data in the yz-plane we rotate the coordinate system about the y-axis keeping y = B until A = -z and C = x (Fig. 5). The hemisphere presented corresponds to $x \leq 0$. Then, setting (A,B,C) = (-z,y,x) and performing the sequence of coordinate transformations discussed above with (A,B,C) replacing (x,y,z), we obtain net coordinates (A,B) representing the yz-plane. Similarly, to view the xz-plane we begin with the axes in the original position (A,B,C) = (x,y,z) and again rotate the coordinate system, this time about the x-axis keeping x = A until B = -z and C = y (Fig. 5). The hemisphere represented by the net corresponds to $y \leq 0$. Setting (A,B,C) = (x,-z,y) and following through the coordinate transformations we obtain net coordinates (A,B) that represent the xz-plane. In these alternate Schmidt nets the trace of the best-fit plane, the pole point, and the linear orientation vector are represented in the (A,B,C) coordinate system and are subject to the requirement $x \leq 0$ or $y \leq 0$.

CONCLUSIONS

A general method has been developed to quantify the planar and/or linear orientation of uniaxial crystals in a sample, leading to an improved understanding of the structure of

the material. The method is the basis of a relatively simple algorithm for computer analysis of large volumes of data. We have emphasized the application of this tool for understanding the structure of ice. The orthogonal least-squares measures of fit presented allow quantitative comparisons between samples and between subsets of the data representing a sample. The capability to view the data and the analytical results on Schmidt nets of different hemispheres provides additional information to improve interpretation by minimizing the importance of net distortion and measurement accuracy limitations.

REFERENCES

Beyer, W.H. (1987) Handbook of Mathematical Sciences, 6th Edition, CRC Press, Inc., Boca Raton, FL.

Claffey, K.J., M.G. Ferrick and J.A. Richter-Menge (1989) "Description of an algorithm and program for ice fabric analysis," USA Cold Regions Research and Engineering Laboratory, CRREL Rept. in prep., Hanover, NH.

Fairbairn, H.W. (1949) Structural Petrology of Deformed Rocks, Addison-Wesley Publishing Company, Inc., Cambridge, MA.

Kamb, W.B. (1962) "Refraction corrections for universal stage measurements I. Uniaxial crystals," The American Mineralogist, Vol. 47, March-April, pp. 227-245.

Knopf, E.B. and E. Ingerson (1938) Structural Petrology, Geological Society of America Memoir 6.

Langway, C.C., Jr. (1958) "Ice fabrics and the universal stage," U.S. Army Snow, Ice and Permafrost Research Establishment Tech. Report 62, 16 pp.

Richter-Menge, J.A., G.F.N. Cox, N. Perron, G. Durell and H.W. Bosworth (1986) "Triaxial testing of first-year sea ice," USA Cold Regions Research and Engineering Laboratory, CRREL Rept. 86-16, Hanover, NH, 41 pp.

Richter-Menge, J.A., G.F.N. Cox and N.M. Perron (1987) "Mechanical properties of multi-year sea ice, Phase I: Ice structure analysis," USA Cold Regions Research and Engineering Laboratory, CRREL Rept. 87-3, Hanover, NH, 30 pp.

Shields, P.C. (1968) Elementary Linear Algebra, Worth Publishers, Inc., New York, NY.

Turner, F.J. and L.E. Weiss (1963) Structural Analysis of Metamorphic Tectonites, McGraw-Hill Book Company, Inc., New York, NY.

Wang, Y.S. (1979) "Crystallographic studies and strength tests of field ice in the Alaskan Beaufort Sea," POAC 79, the Fifth International Conference on Port and Ocean Engineering under Arctic Conditions, Proceedings Vol. 1, pp. 651-665.

Weeks, W.F. and S.F. Ackley (1982) "The growth, structure and properties of sea ice," USA Cold Regions Research and Engineering Laboratory, CRREL Monograph 82-1, Hanover, NH, 130 pp.

Weeks, W.F. and A.J. Gow (1978) "Preferred crystal orientations along the margins of the Arctic Ocean," Journal of Geophysical Research, Vol. 84, pp. 5105-5121.